NAVAL POSTGRADUATE SCHOOL

MONTEREY, CALIFORNIA

THESIS

COHERENT NOISE REJECTION IN A THREE-PHASE POWER INVERTER

by

Daniel G. Wheaton

June 2011

Thesis Co-Advisors: Roberto Cristi
                           Alexander Julian

Approved for public release; distribution is unlimited

THIS PAGE INTENTIONALLY LEFT BLANK

REPORT DOCUMENTATION PAGE		*Form Approved OMB No. 0704-0188*
Public reporting burden for this collection of information is estimated to average 1 hour per response, including the time for reviewing instruction, searching existing data sources, gathering and maintaining the data needed, and completing and reviewing the collection of information. Send comments regarding this burden estimate or any other aspect of this collection of information, including suggestions for reducing this burden, to Washington headquarters Services, Directorate for Information Operations and Reports, 1215 Jefferson Davis Highway, Suite 1204, Arlington, VA 22202-4302, and to the Office of Management and Budget, Paperwork Reduction Project (0704-0188) Washington DC 20503.		
1. AGENCY USE ONLY *(Leave blank)*	**2. REPORT DATE** June 2011	**3. REPORT TYPE AND DATES COVERED** Master's Thesis
4. TITLE AND SUBTITLE Coherent Noise Rejection in a Three-Phase Power Inverter		**5. FUNDING NUMBERS** N/A
6. AUTHOR(S) Daniel G. Wheaton		
7. PERFORMING ORGANIZATION NAME(S) AND ADDRESS(ES) Naval Postgraduate School Monterey, CA 93943-5000		**8. PERFORMING ORGANIZATION REPORT NUMBER**
9. SPONSORING /MONITORING AGENCY NAME(S) AND ADDRESS(ES) N/A		**10. SPONSORING/MONITORING AGENCY REPORT NUMBER**
11. SUPPLEMENTARY NOTES The views expressed in this thesis are those of the author and do not reflect the official policy or position of the Department of Defense or the U.S. Government. IRB Protocol number _____N.A._____.		
12a. DISTRIBUTION / AVAILABILITY STATEMENT Approved for public release; distribution is unlimited		**12b. DISTRIBUTION CODE** A

13. ABSTRACT (maximum 200 words)

In this thesis, we discuss the design of a controller to reject the effects of high order harmonics in a three-phase power inverter. Specifically, coherent noise in the fifth harmonic is considered, as it seems to be dominant in most applications. The controller used in this power inverter operates in a reference frame synchronous with the 60 Hz line voltage. This transformation effectively changes the desired 60 Hz sine wave output into a DC value that has the same amplitude as the sine wave. The power inverter uses an optimal form of pulse-width modulation (PWM), called space vector modulation, which causes the harmonic noise.

In order to reject the distortions introduced by the space-vector modulation process, a Linear Quadratic Gaussian (LQG) controller is designed with the sinusoidal disturbances modeled as uncontrollable modes of the system, which are observable from the input and output signals.

The extra states in the state space model associated with the disturbance are estimated by the Kalman Filter and subtracted from the control input to compensate for the disturbance.

14. SUBJECT TERMS Pulse Width Modulation (PWM), Linear Quadratic Regulator (LQR), Linear Quadratic Gaussian Controller (LQG), Coherent Noise Rejection			**15. NUMBER OF PAGES** 55
			16. PRICE CODE
17. SECURITY CLASSIFICATION OF REPORT Unclassified	**18. SECURITY CLASSIFICATION OF THIS PAGE** Unclassified	**19. SECURITY CLASSIFICATION OF ABSTRACT** Unclassified	**20. LIMITATION OF ABSTRACT** UU

NSN 7540-01-280-5500

Standard Form 298 (Rev. 2-89)
Prescribed by ANSI Std. 239-18

THIS PAGE INTENTIONALLY LEFT BLANK

COHERENT NOISE REJECTION IN A THREE-PHASE POWER INVERTER

Daniel G. Wheaton
Ensign, United States Navy
B.S., United States Naval Academy, 2010

Submitted in partial fulfillment of the
requirements for the degree of

MASTER OF SCIENCE IN ELECTRICAL ENGINEERING

from the

**NAVAL POSTGRADUATE SCHOOL
June 2011**

Author: Daniel G. Wheaton

Approved by: Dr. Roberto Cristi
       Thesis Co-Advisor

       Dr. Alexander L. Julian
       Thesis Co-Advisor

       Dr. Clark Robertson
       Chair, Department of Electrical and Computer Engineering

THIS PAGE INTENTIONALLY LEFT BLANK

ABSTRACT

In this thesis, we discuss the design of a controller to reject the effects of high order harmonics in a three-phase power inverter. Specifically, coherent noise in the fifth harmonic is considered, as it seems to be dominant in most applications. The controller used in this power inverter operates in a reference frame synchronous with the 60 Hz line voltage. This transformation effectively changes the desired 60 Hz sine wave output into a DC value that has the same amplitude as the sine wave. The power inverter uses an optimal form of pulse-width modulation (PWM), called space vector modulation, which causes the harmonic noise.

In order to reject the distortions introduced by the space-vector modulation process, a Linear Quadratic Gaussian (LQG) controller is designed with the sinusoidal disturbances modeled as uncontrollable modes of the system, which are observable from the input and output signals.

The extra states in the state space model associated with the disturbance are estimated by the Kalman Filter and subtracted from the control input to compensate for the disturbance.

THIS PAGE INTENTIONALLY LEFT BLANK

TABLE OF CONTENTS

THIS PAGE INTENTIONALLY LEFT BLANK

LIST OF FIGURES

THIS PAGE INTENTIONALLY LEFT BLANK

LIST OF ACRONYMS AND ABBREVIATIONS

PWM   Pulse Width Modulation

PI   Proportional Integral

LQG   Linear Quadratic Gaussian regulator

qd0   Synchronous Reference Frame

LQR   Linear Quadratic Regulator

THIS PAGE INTENTIONALLY LEFT BLANK

EXECUTIVE SUMMARY

Modern shipboard equipment requires a variety of power and provides a variety of power sources. As these systems become increasingly complex, it is crucial that conversion from one type of power to the other be efficient and cost effective. The use of an active control loop to reject harmonic noise in a three-phase power inverter, thus reducing total harmonic distortion using digital methods, without adding significant hardware to the inverter is examined in this thesis.

Typically, power inverters convert DC power to an AC waveform using pulse-width modulation, which is a form of timed on/off switching. Since this switching action provides a square wave-like input, harmonic noise is generated. The traditional method of preventing this noise from directly affecting the load is to add a passive filter whose power absorption may not be negligible. By applying modern control theory to this problem, harmonic noise can be more completely rejected, providing a more robust overall system at a lower cost.

A Linear Quadratic Gaussian (LQG) regulator is used in this thesis with a modified Kalman filter. The system was designed to reject noise at specific frequencies, and the fifth harmonic was rejected in this case. To modify the Kalman filter, states were added estimating the sinusoidal disturbances. These estimates were then subtracted from the final input, cancelling any input disturbance.

The modified LQG controller was simulated using Simulink and performed well under circumstances of fairly low signal-to-noise ratio. Without additive white Gaussian noise and in steady state, the controller completely rejected the fifth harmonic coherent noise. As the power of the white noise increases, system performance begins to degrade. It is expected that this controller will perform well within military specifications in a real-world implementation.

This is a preliminary simulation study of this problem. It is intended to be followed by further study into the possibility of implementation on a Field Programmable Gate Array (FPGA) for real-time applications to a power inverter.

The simulations provided demonstrate the feasibility of effectively rejecting coherent noise in a power inverter using a closed loop, active control scheme instead of a large passive filter. This is desirable in situations where a passive filter requires expensive components or lots of space.

ACKNOWLEDGMENTS

Dr. Roberto Cristi
Thesis Co-Advisor

Dr. Alexander Julian
Thesis Co-Advisor

THIS PAGE INTENTIONALLY LEFT BLANK

I. INTRODUCTION

A. BACKGROUND

Three-phase power inverters take DC current and convert it to three-phase AC current. This has many applications in modern electronics and shipboard electrical systems, such as powering a radar unit that requires three-phase power from a DC bus. One increasingly common method for controlling the AC current delivered to a load is space vector modulation, which is an optimal method of pulse-width modulation (PWM) [1]. This method results in a sinusoidal current that has been generated from timed switching and always yields harmonic noise disturbance at the final output. These higher order harmonics are undesirable in many applications where steady AC power is required at the load. For example, harmonics in an inverter that is being used to power a piece of machinery aboard a submarine could translate into harmonics in the physical drive of that machinery. This could result in undesirable structural noise emitted into the environment at specific harmonic frequencies.

B. MOTIVATION

Power inversion is commonly used on shipboard systems to run three-phase machinery. Specific requirements for all shipboard electrical devices are stated in Military Standard 1399 [2]. This standard specifies that total harmonic distortion for electrical power systems is limited to five percent maximum, with three percent maximum due to a single harmonic [2]. The common solution to minimize harmonic distortion has been to add a filter with a large capacitor. This passive solution is expensive and hardware intensive. With today's modern technology, an active harmonic rejection system using digital power control is feasible and affordable. As the Navy's power demands increase, the efficiency and cost of electronic conversion devices needs to be reduced. A digital method of actively rejecting harmonic noise in power conversion is discussed in this thesis.

1

C.   PROBLEM STATEMENT

The basic layout of the physical system is shown in Figure 1; harmonic noise is injected at the output of the inverter, entering the load (L_o , R_o) as a result of the space vector modulation. In this case, the fifth harmonic is the tone that will be rejected as it is the first major harmonic generally seen in power inverters. The method discussed in this thesis can be used to reject any harmonic or any number of harmonics. The direction of current flow and bias of voltages for each of the three phases is shown in Figure 1.
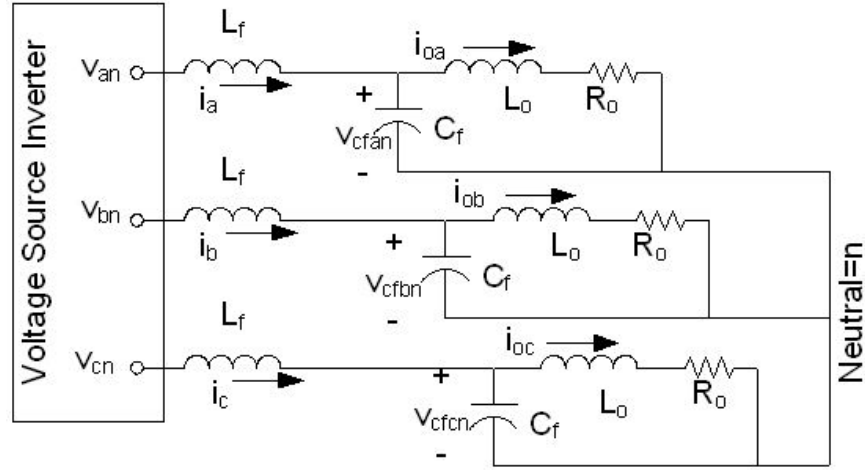

Figure 1.   A layout of the physical system.

Currently, the most common approach for active sinusoid rejection is based on two cascaded proportional integral (PI) controllers as shown in Figure 2. The system block represents the physical system shown in Figure 1. The entire control system operates in a synchronous reference frame, which effectively transforms the 60 Hz three-phase currents (called "abc" components), into DC values (called "qd0" components) depending on the magnitude and phase of the original currents [3]. The asterisks in Figures 2 and 3 represent desired values for their related currents and voltages in the system. Voltages and currents represented with subscripts are the voltages and currents corresponding to the phase of the subscript. The subscript "qds" represents a vector containing all of the values for the current or voltage in the "qd0" reference frame. V_{cf} represents the capacitor voltages at the load, as defined in Figure 1.
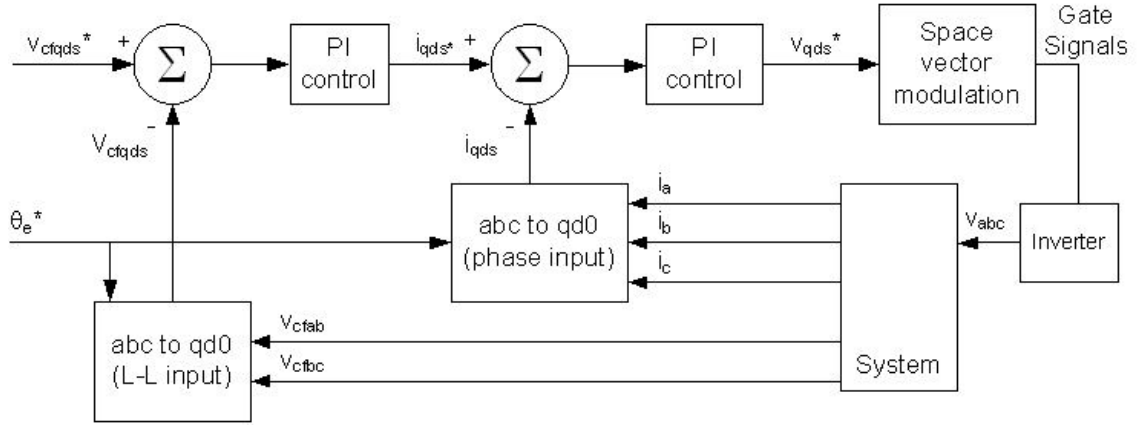
2

Figure 2.   Cascaded PI controllers in their current configuration.

In this thesis, the two PI controllers are replaced with a single linear quadratic Gaussian regulator (LQG) specifically tuned to reject sinusoidal disturbances of given frequencies. The goal is to use the flexibility of the LQG controller and its ability to incorporate mathematical disturbance models in order to achieve a better performance. The proposed control system layout is shown in Figure 3, where the LQG controller rejects harmonic noise at the input of the plant, or system, in Figure 3.
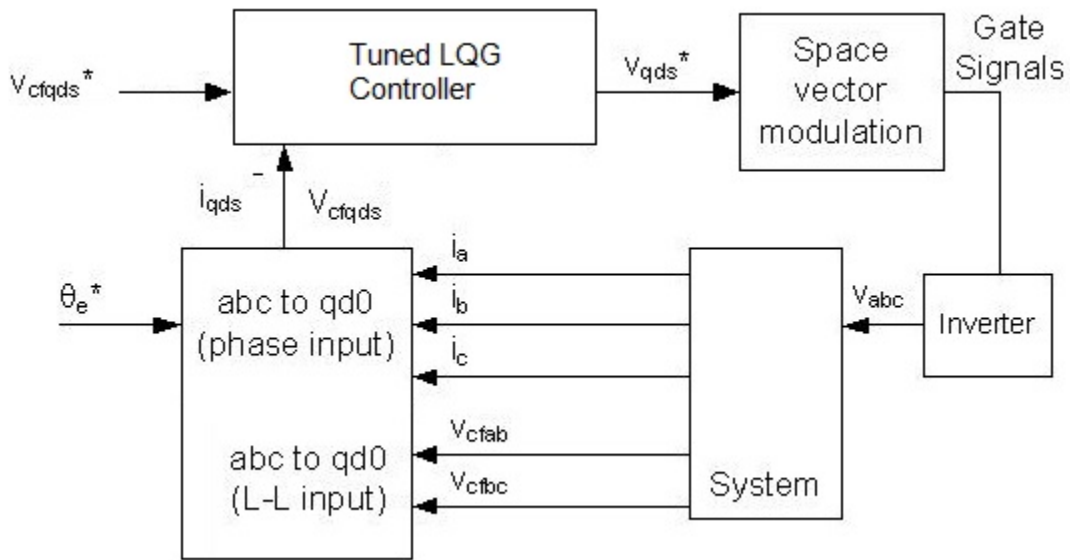

Figure 3.   Proposed LQG controller for improved harmonic noise rejection.

3

In order to effectively develop and test a controller for this plant (physical system), a mathematical model describing the dynamics of the plant must be created. The plant model is derived from the physical properties of the electrical components shown in Figure 1. Differential equations must be derived to solve for the inductor currents, capacitor voltages and load currents in the synchronous (qd0) reference frame. The differential equations for the filter inductor currents in their "qd0" components are [4]

$$sL_f \begin{bmatrix} i_{qs} \\ i_{ds} \end{bmatrix} + \omega L_f \begin{bmatrix} 0 & 1 \\ -1 & 0 \end{bmatrix} \begin{bmatrix} i_{qs} \\ i_{ds} \end{bmatrix} + \begin{bmatrix} v_{cfqs} \\ v_{cfds} \end{bmatrix} - \begin{bmatrix} v_{qs} \\ v_{ds} \end{bmatrix} = 0 \tag{1}$$

Similarly, the "qd0" differential equations describing capacitor voltages are [4]

$$sC_f \begin{bmatrix} v_{cfqs} \\ v_{cfds} \end{bmatrix} + \omega C_f \begin{bmatrix} 0 & 1 \\ -1 & 0 \end{bmatrix} \begin{bmatrix} v_{cfqs} \\ v_{cfds} \end{bmatrix} + \begin{bmatrix} i_{oqs} \\ i_{ods} \end{bmatrix} - \begin{bmatrix} i_{qs} \\ i_{ds} \end{bmatrix} = 0 \tag{2}$$

Finally, the load inductor currents can be described as [4]

$$sL_o \begin{bmatrix} i_{oqs} \\ i_{ods} \end{bmatrix} + \omega L_o \begin{bmatrix} 0 & 1 \\ -1 & 0 \end{bmatrix} \begin{bmatrix} i_{oqs} \\ i_{ods} \end{bmatrix} + R_o \begin{bmatrix} i_{oqs} \\ i_{ods} \end{bmatrix} - \begin{bmatrix} v_{cfqs} \\ v_{cfds} \end{bmatrix} = 0 \tag{3}$$

These currents and voltages are the "qd0" currents and voltages that define the system shown in Figure 1. Combining these equations into a single, state space model of the form $Mx + sNx + Pu = 0$ as shown in (4), we get

$$\begin{bmatrix} 0 & \omega L_f & 1 & 0 & 0 & 0 \\ -\omega L_f & 0 & 0 & 1 & 0 & 0 \\ -1 & 0 & 0 & \omega C_f & 1 & 0 \\ 0 & -1 & -\omega C_f & 0 & 0 & 1 \\ 0 & 0 & -1 & 0 & R_o & \omega L_o \\ 0 & 0 & 0 & -1 & -\omega L_o & R_o \end{bmatrix} \begin{bmatrix} i_{qs} \\ i_{ds} \\ v_{cfqs} \\ v_{cfds} \\ i_{oqs} \\ i_{ods} \end{bmatrix} + s \begin{bmatrix} L_f & 0 & 0 & 0 & 0 & 0 \\ 0 & L_f & 0 & 0 & 0 & 0 \\ 0 & 0 & C_f & 0 & 0 & 0 \\ 0 & 0 & 0 & C_f & 0 & 0 \\ 0 & 0 & 0 & 0 & L_o & 0 \\ 0 & 0 & 0 & 0 & 0 & L_o \end{bmatrix} \begin{bmatrix} i_{qs} \\ i_{ds} \\ v_{cfqs} \\ v_{cfds} \\ i_{oqs} \\ i_{ods} \end{bmatrix} - \begin{bmatrix} v_{qs} \\ v_{ds} \\ 0 \\ 0 \\ 0 \\ 0 \end{bmatrix} = 0 \tag{4}$$

Equation (4) can then be put in the standard state space format $\dot{x} = Ax + Bu$:

$$A = -N^{-1}M \tag{5}$$

$$B = -N^{-1}P \tag{6}$$

4

The matrix N is always invertible and well conditioned, thus, a six-state, standard form state space equation can be derived [4]. Using this plant model, a controller can be designed and simulated.

Since the phase of the 60 Hz reference frame can be chosen arbitrarily, it is customary to choose it so that one or more of the voltages or current components are zero. In this case, we chose it so that the DC input voltage on the first capacitor as a "q" component v_{cfqs} equal to 480 V (in the "qd0" reference frame) while the "d" component v_{cfds} and the "0" component are set to 0 V. A simple feedback gain controller is all that is required to maintain a steady output of 480 V in ideal circumstances. However, due to external disturbances and harmonics due to switching, this plant receives a non-ideal input, with both white noise due to sensors and real components and significant coherent noise due to space vector modulation. A more complex controller is, therefore, needed to maintain a steady output voltage in the "qd0" reference frame.

D.   PROPOSED SOLUTION

The LQG controller is designed as an optimal controller, which is inherently robust in the presence of white noise, and does not require the ability to directly measure all of the plant states [5]. In this particular plant, there are sensors that allow us to indirectly measure i_{qs}, i_{ds}, v_{cfqs}, and v_{cfds}, the first four states of the six-state system. Since the controller is fully defined in the reference frame, all measured currents and voltages are converted from the triphase "abc" components to the "qd0" components by well-defined matrix transformations [3]. In general, all currents and voltages are balanced, and the "0" component can be set to zero a priori. These measurements are accomplished by measuring the states' related values in the absolute reference frame and mathematically transforming them into the qd0 reference frame. The Kalman filter in the LQG controller takes these measurements and estimates the other two states, which can then be fed back to the controller.

Along with its inherent robustness in the presence of white noise, the LQG controller was also selected because of its ability to estimate the effects of various disturbances with its Kalman filter. This filter can be modified to reject specific

frequencies at the input, which is ideal for coherent noise at known frequencies. A specific design of the controller to reject the harmonic disturbances is presented in the next chapter.

E.   THESIS ORGANIZATION

This thesis is organized as follows. The main structure of the controller is shown in Chapter II, where all relevant state space equations of the system are derived. The methods used in simulation are described in Chapter III, while the simulation results are in Chapter IV. Finally, the conclusion of the research and recommendations for possible directions for further research are in Chapter V.

II. CONTROLLER

A. LQG CONTROL

The LQG controller is a combination of the Linear Quadratic Regulator (LQR) and a Kalman filter. Both the LQR and the Kalman filter are an optimization of a cost function, and have some degree of optimality that makes them very desirable solutions. Therefore, the combination of these two techniques also yields an optimal controller based on what is known as the principle of separation [5].

1. LQR Controller

The linear quadratic regulator is a controller designed to provide the optimum control gain K to feed back the system states. The LQR's defining cost function is defined as [5]

$$J = \int_0^{t_f} \left(x^T Q x + u^T R u \right) dt \tag{7}$$

In Equation (7), the parameters Q and R are set by the control designer and represent the weights given to plant states and control input, respectively. A Q that is much larger than R represents the designer's desire for the system to reach the desired output states quickly without regard for control effort. Conversely, a very small Q relative to R represents a controller that gradually reaches the desired output while minimizing control effort. In this thesis, the Q matrix was given five times the weight of the R matrix. If a faster response time is required, this ratio can be increased.

The solution to the LQR cost function results in a feedback gain that minimizes J. If the controller is intended to run for extended periods of time, the steady-state solution is obtained by assuming t_f to be infinity, resulting in constant feedback gains. In this case, the solution that minimizes J is defined by the steady-state Riccati equations [5]

$$PA + A^T P - PBR^{-1}B^T P + Q = 0 \tag{8}$$

$$K = R^{-1}BP \tag{9}$$

Thus, the optimal system input is $u = -Kx(t)$.

In order to drive the filter capacitor voltages in the power inverter to a desired input, and not simply to zero as an LQR does, the corresponding states x_3 and x_4, or the third and forth states in the six-state system, are replaced by the error with respect to the desired set-points. As $x_3 = x_3 - x_{3Desired}$ it turns out that by the inclusion of one or more integrators, the desired values are represented by the initial conditions of the integrators themselves. In this way, minimizing a weighted magnitude of the overall state corresponds to a minimal tracking error.

This controller has the disadvantage of requiring full informational feedback to work. Since all six plant states cannot be directly measured, an estimate of the vector $x(t)$ must be generated. This is done using a Kalman filter.

2.   The Kalman Filter

The state variables of a system are estimated by the Kalman filter according to

$$\dot{\hat{x}}(t) = A\hat{x}(t) + B_u u(t) + G[m(t) - C_m \hat{x}(t)] \quad (10)$$

In Equation (10), G is called the Kalman gain, which multiplies the error between the measured states of the system and its estimated states. The Kalman gain is selected as the solution that minimizes the mean-square error

$$J = E\left[\{x(t) - \hat{x}(t)\}^T \{x(t) - \hat{x}(t)\} \right] \quad (11)$$

where $\hat{x}(t)$ is the estimated state. Mean-square error is minimized by solving the steady-state Riccati equation in a manner similar to that used for the LQR. In this case, the C matrix (from the original state space model) is used, and W and V are selected as the weights on plant and sensor noise respectively. The observer gain is given by [5]

$$PA + A^T P - PC^T V^{-1} CP + W = 0 \quad (12)$$
$$G = PC^T V^{-1} \quad (13)$$

What is important here is that the two sets of covariance matrices W and V can be used to shape the response in a desired fashion. In particular, selecting values of W to be much larger than V results in a system that is less sensitive to measurement noise from the

8

sensors and relies more on the dynamic model of the system. Similarly, selecting values of W much smaller than V allows for more uncertainties in the plant model but more precise sensors measuring the actual states in the system. The plant model used in this thesis is derived from well known differential equations on a system with high-quality electrical components; therefore, the values of the measurement noise covariance matrix W are much larger than the values of the system noise covariance matrix V, making the system less sensitive to measurement noise.

3. LQG Control

The concepts of the LQR controller and the Kalman filter can be combined as one system with the estimated state vector $\hat{x}(t)$ fed back to the LQR controller, resulting in the final input equation $u(t) = -K\hat{x}(t)$. This system provides a robust controller that is well suited to be modified to reject coherent noise.

B. SINUSOID REJECTION

The LQG controller assumes a linear state-space model $\dot{x} = Ax + Bu$ for the plant. In this particular application, it is assumed that there is a disturbance at the input due to switching currents. Therefore, the state space-equation describing this system is modified to

$$\dot{x} = Ax + B(u + s) \tag{14}$$

where s is a sinusoidal disturbance of known frequency but unknown amplitude or phase. Because s is sinusoidal, its second time derivative is given by

$$\ddot{s} = -\omega^2 s \tag{15}$$

Using Equation (15), we define a full state definition for s as

$$\begin{bmatrix} \dot{s} \\ \ddot{s} \end{bmatrix} = \dot{x}_s = \begin{bmatrix} 0 & 1 \\ -\omega^2 & 0 \end{bmatrix} x_s = A_s x_s \tag{16}$$

Substituting Equation (16) into (14), we get

9

$$\dot{x} = Ax + Bu + B\left\{\begin{pmatrix} 0 & 1 \end{pmatrix} x_{s1} + \begin{pmatrix} 0 & 1 \end{pmatrix} x_{s2} + \ldots \right\} \tag{17}$$

where a new x_s term is added for each frequency to be rejected. With the disturbance defined as in Equation (17), both plant and disturbance dynamics can be described by one single state-space model that combines all the states (plant and disturbance) of the system. Since there are two distinct inputs, one for the "q" and one for the "d" components and each sinusoid represents two states, there is a total of an additional four states associated to each sinusoidal disturbance. This can be written as

$$\begin{pmatrix} \dot{x}_{sq} \\ \dot{x}_{sd} \\ \dot{x} \end{pmatrix} = \begin{pmatrix} A_s & 0 & 0 \\ 0 & A_s & 0 \\ [\bar{B}] & & A \end{pmatrix} \begin{pmatrix} x_{sq} \\ x_{sd} \\ x \end{pmatrix} + \begin{pmatrix} 0 \\ 0 \\ B \end{pmatrix} u \tag{18}$$

where x_{sq} and x_{sd} represent the disturbance states on the "q" and "d" components and $\begin{bmatrix} \bar{B} \end{bmatrix}$ represents the disturbance's impact on the plant states. For one sinusoid $\begin{bmatrix} \bar{B} \end{bmatrix}$ is defined as

$$\begin{bmatrix} \bar{B} \end{bmatrix} = B \begin{bmatrix} 0 & 1 & 0 & 0 \\ 0 & 0 & 0 & 1 \end{bmatrix}. \tag{19}$$

The new state equation given in (18) describes a system with all of the previous plant dynamics, as well as four new states, describing the value and time derivative of the sinusoidal disturbances for each system input. In the Kalman filter, the plant states are fed back through the feedback gain K as defined by the LQR controller. The x_s states estimating the disturbance sinusoids are subtracted from the system input, effectively cancelling the disturbance. The commanded signal leaving the controller is

$$u(t) = -K\hat{x}(t) - \begin{bmatrix} 0 & 1 \end{bmatrix} \hat{x}_s(t). \tag{20}$$

This method allows the system to reject a sinusoidal disturbance of known frequency regardless of amplitude or phase. The Kalman filter accurately estimates the disturbance and compensates for it at the input to the plant. If a disturbance with more than one frequency is to be rejected, this can be accomplished simply by adding additional states in the same manner shown above.

One drawback to this method is that the Kalman filter is computationally intensive. The power inverter simulated in this thesis, rejecting two sinusoids, has an A matrix that has dimensions 14 by 14. However, the overall dynamic model can be implemented in a number of transfer functions and the complexity greatly reduced. Also, model reduction techniques can be employed to reduce the order of the controller. However, this is beyond the scope of this thesis.

C.   TIME DELAY COMPENSATION

In most applications, the time latency due to computation time must be taken into account. The computational delay can be modeled as a delay at the output of the controller of the form e^{-sT}, an ideal time delay the Laplace domain. Since the computational delay is quite small, (on the order of 100 microseconds,) e^{-sT} can be approximated as

$$e^{-sT} \approx \frac{1 - s\dfrac{T}{2}}{1 + s\dfrac{T}{2}} \tag{21}$$

The approximation shown in Equation (21) has the advantage that it has exact unit magnitude and a fairly linear phase, at least at low frequencies. Also, since it is a linear time-invariant system, it is easily modeled by an extra state of the overall system. In order to determine a state space model, we can write the transfer function due to the time delay as

$$V(s) = \left(\frac{1 - s\dfrac{T}{2}}{1 + s\dfrac{T}{2}} \right) U(s) \tag{22}$$

where $V(s)$ is the Laplace transform of the delayed input signal to the plant. Manipulating Equation (22), we get

$$V(s) = -U(s) + \left(\frac{\dfrac{4}{T}}{s + \dfrac{2}{T}} \right) U(s) \tag{23}$$

.

Converting the previous equation from the frequency domain into the time domain, we get the following state space model for the time delay:

$$\dot{z}(t) = -\frac{2}{T} z(t) + \frac{4}{T} u(t) \tag{24}$$

and

$$v(t) = z(t) - u(t) \tag{25}$$

Equations (24) and (25) can be applied to the state space model in the Kalman filter to compensate for the computational time delay T. By incorporating the state in the overall state space model as

$$\dot{x}(t) = Ax(t) + B(z(t) - u(t)) \tag{26}$$

the $z(t)$ term can be forwarded into the system A matrix in a method similar to that used for the sinusoidal rejection, hence,

$$\begin{bmatrix} \dot{x} \\ \dot{z}_1 \\ \dot{z}_2 \end{bmatrix} = \begin{bmatrix} A & B \\ -\dfrac{2}{T} & 0 & 0 \\ 0 & -\dfrac{2}{T} & 0 \end{bmatrix} \begin{bmatrix} x \\ z_1 \\ z_2 \end{bmatrix} + \begin{bmatrix} -B \\ \dfrac{4}{T} & 0 \\ 0 & \dfrac{4}{T} \end{bmatrix} u \tag{27}$$

the state is added twice, once for the "q" and once for the "d" component as z_1 and z_2. These states are fed back through the LQR gain as though they were a part of the plant. This method compensates for a time delay as long as the delay length T is known.

III.   SIMULATION

The entire system was modeled in Simulink, which provided a test bed for quick modification and experimentation of the system. Simulink is ideal for performing high-level computer simulations of dynamic systems. The overall system architecture, shown in Appendix A, contains three primary subsystems: a plant subsystem, an observer subsystem, and a controller subsystem. Disturbances and measurement noises are added externally. All the model parameters are defined in an initialization function, which is provided in Appendix B. All subsystems are described in the remainder of this chapter.

A.   PLANT DYNAMICS

The plant subsystem models the dynamics of the inverter as discussed in Section 1C. The differential equations are in state space form $\dot{x} = Ax + Bu$ and are shown in detail in Figure 4.

Figure 4.   Plant dynamics subsystem Simulink model.

As stated in Section 1C, the dynamic equations of the inverter are derived from nodal equations. This subsystem accurately models the dynamic plant behavior but does not include external disturbances. Figure 4 is a representation of an idealized version of the inverter.

B.   OBSERVER

The observer subsystem, similar to the plant subsystem, is represented by the mathematical equations that define the Kalman filter:

$$\dot{\hat{x}}(t) = A\hat{x}(t) + B_u u(t) + G[m(t) - C_m \hat{x}(t)] \tag{28}$$
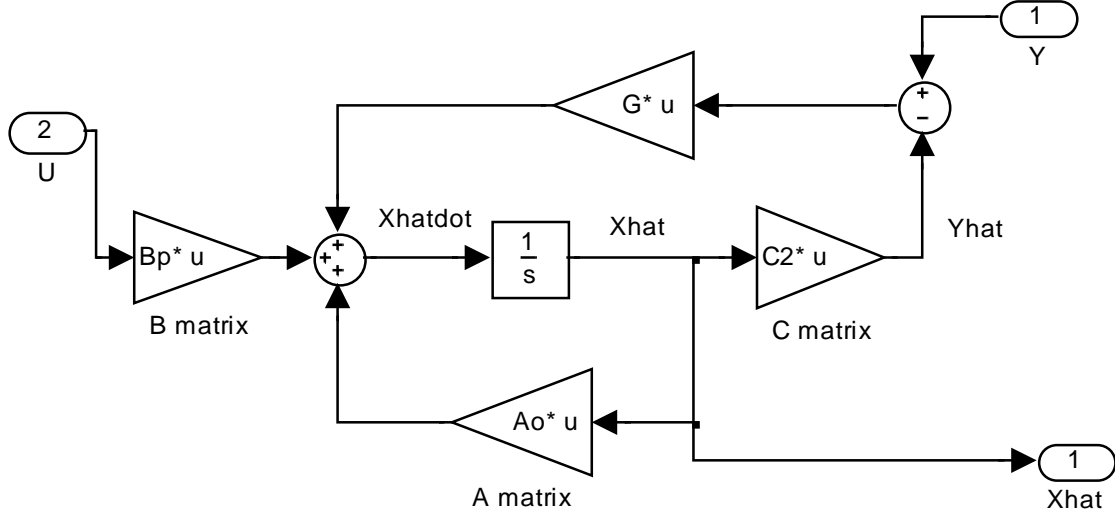
The observer subsystem is shown in detail in Figure 5.

Figure 5.   Observer subsystem schematic Simulink model.

Notice that the A and B in the dynamic model of the observer have been replaced with A_o and Bp, respectively. These matrices include the plant dynamics and the dynamics of the sinusoidal disturbances. See Appendix B for detailed definitions of the matrices used in Simulink. This results in additional states for the Kalman filter so the disturbances can be estimated as part of the new augmented state. The matrices are given by Equation (18) in Section 2b.

C.   CONTROLLER

The controller subsystem takes the estimated state vector from the Kalman filter and applies the appropriate LQR gains to the states associated with the plant and time delay. Its schematic is shown in Figure 6.
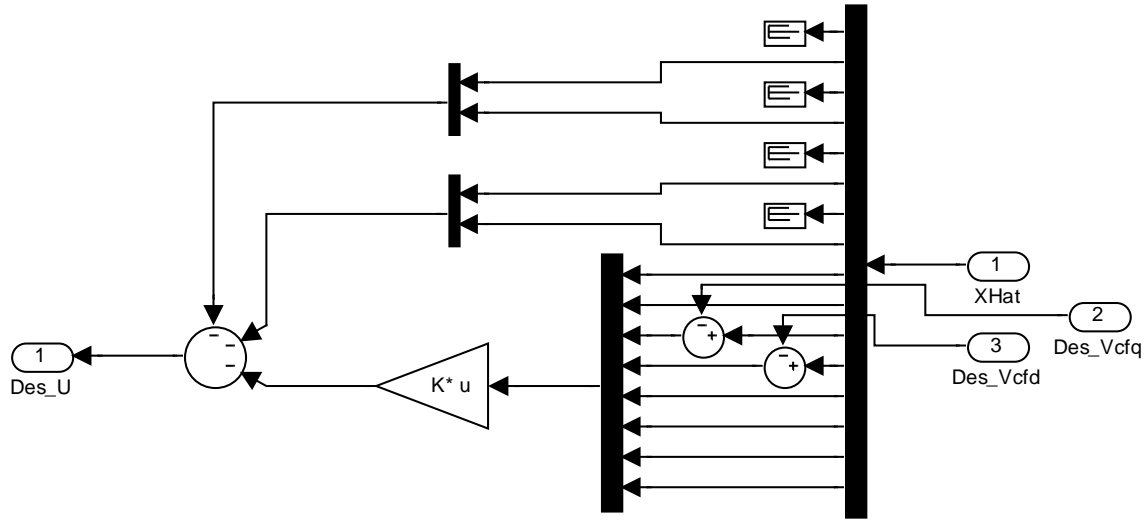
Figure 6.   Controller subsystem schematic Simulink model.

Note that the third and fourth states have a value subtracted from them. These states represent the capacitor voltages over which control is desired. By subtracting the desired value, those states become an "error" term and, as they are driven to zero, the actual capacitor value is driven to the desired capacitor value. The top eight states represent the sinusoidal disturbance estimates. The derivatives are not used, but their actual values are multiplexed into a vector to match the system input size and subtracted from the input. This effectively cancels the disturbance input, which is added at the input to the plant dynamics subsystem.

THIS PAGE INTENTIONALLY LEFT BLANK

IV. RESULTS

A. FULL FEEDBACK LQR CONTROL

The first control attempt was a full state feedback control, where it is assumed that all currents and voltages are available for measurements. This was to validate the controller in the absence of noise due to either disturbances or induced because of the estimator. The results are shown in Figure 7.
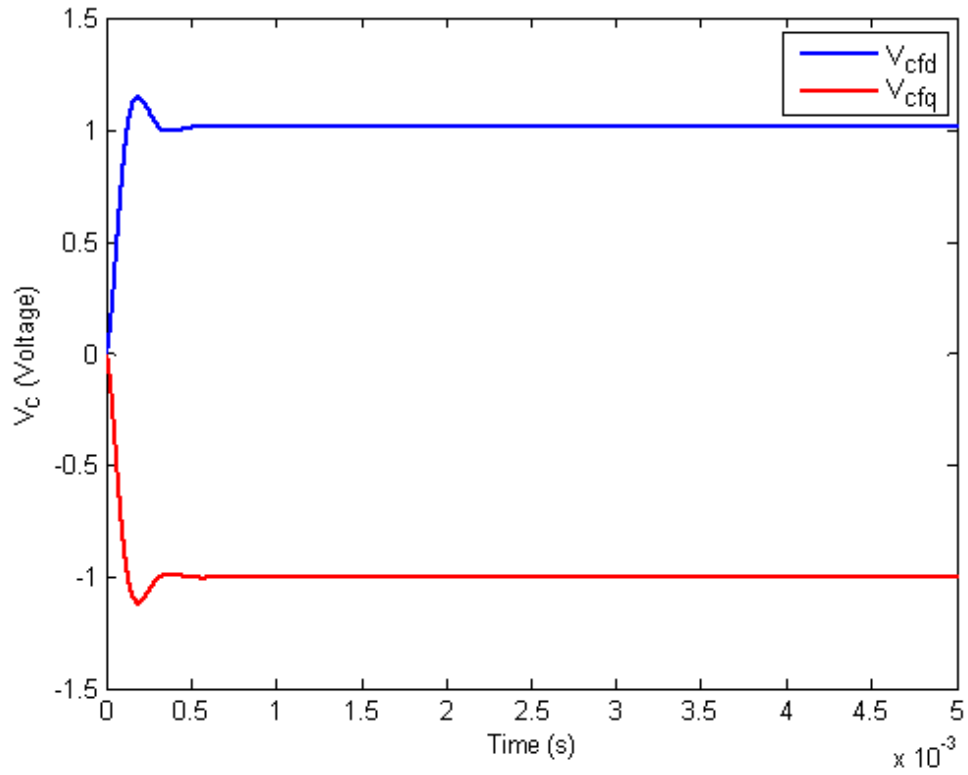

Figure 7. Full informational control.

Note this system has a very rapid settling time of less than half a millisecond. For this simulation, the desired capacitor voltages were arbitrarily set to one and negative one for the purpose of demonstrating independent control of both states.

According to the applications, we can vary the dynamics of the controller to accommodate a number of requirements. In practical applications, all voltages and

currents must be within certain limits to avoid saturations and overload. By the optimal controller, the parameters Q and R in the cost function (Equation [7]) can be varied to shift the cost from the control signal to the states. An increase in the penalty on the control signal clearly results in a less demanding control effort which, in many cases, prevents the system from going into saturation.

B.   NOISELESS LQG CONTROL

After the controller was validated, a Kalman filter was added and tested with a small discrepancy in initial value. The result is shown in Figure 8, where one capacitor voltage was commanded to 480 V and one to 0 V.
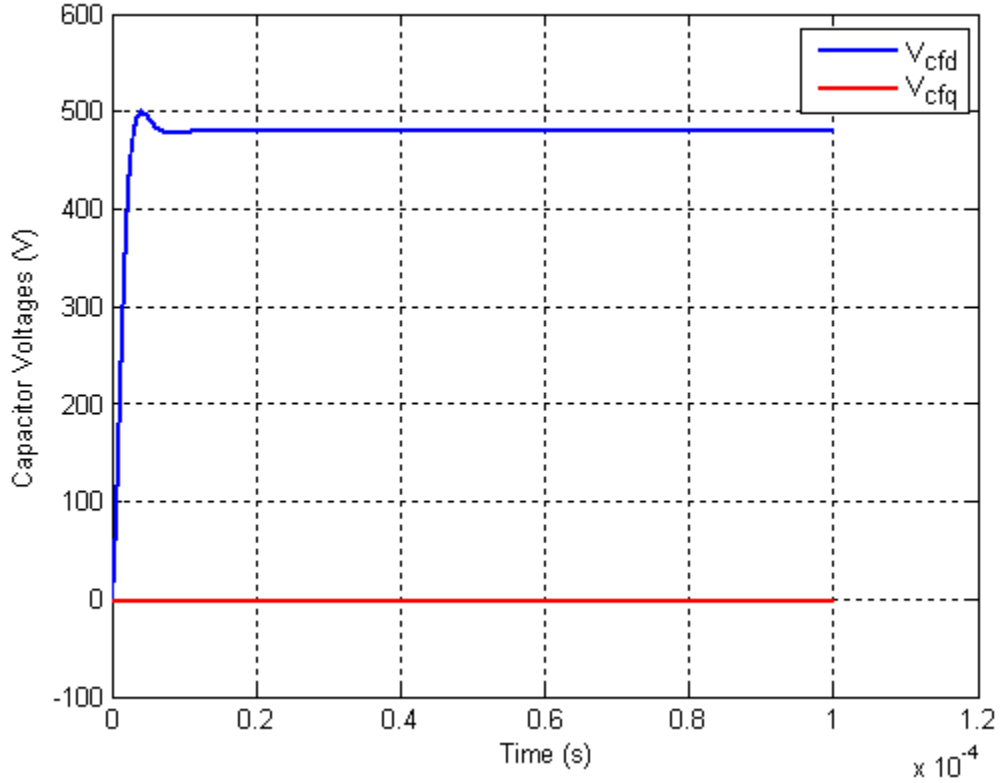

Figure 8.   Capacitor voltages: LQG control.

The estimated V_{cfd} converges to the actual V_{cfd} in the Kalman filter, as can be seen in Figure 9.
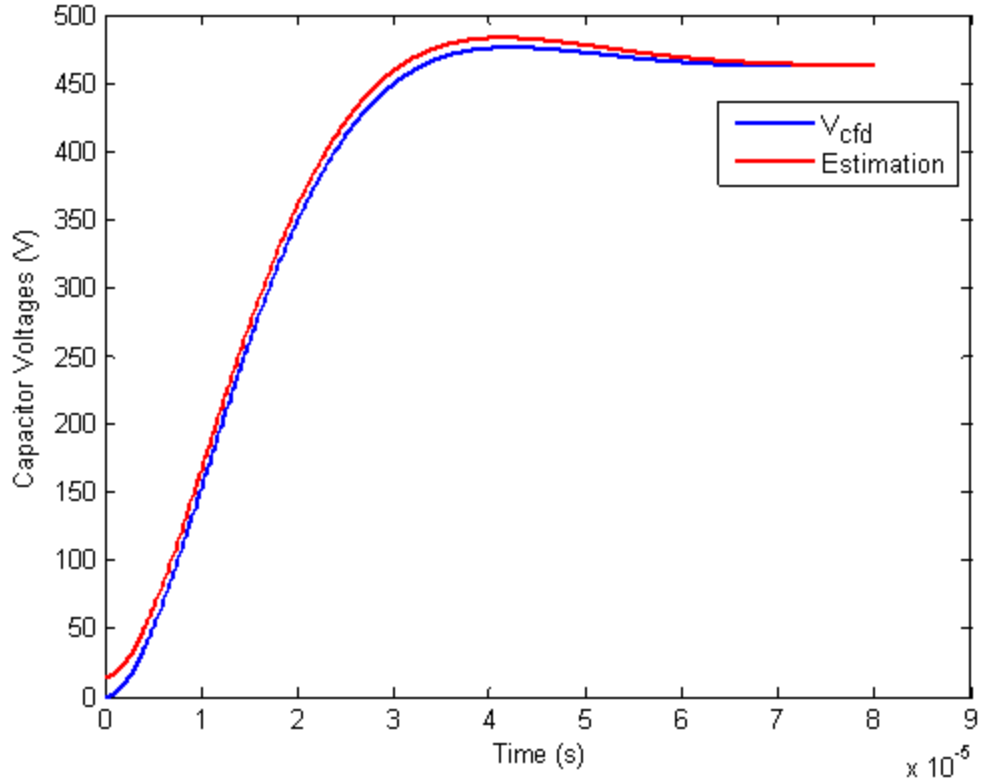
18

Figure 9.   Kalman estimation converging with V_{cfd}.

Depending on the parameters set in the Kalman filter, the estimated states converge to the actual states very quickly. This causes the system to behave effectively as though it has full informational control.

The attractive feature of the Kalman Filter, which is particularly advantageous in this implementation, is the fact that modeling errors can be modeled by what is called the "system noise" at the input of the state equations. The estimates can be made less sensitive to parameters' uncertainties by changing the covariance of this noise.

C.   LQG CONTROL WITH COHERENT NOISE

When two sinusoidal states are added to the Kalman filter, and the associated frequency disturbances are added as described in Section II.B, the system response remains very good, as shown in Figure 10. Without the presence of white noise, the estimated sinusoids perfectly cancel the coherent disturbance within 2.5 milliseconds.
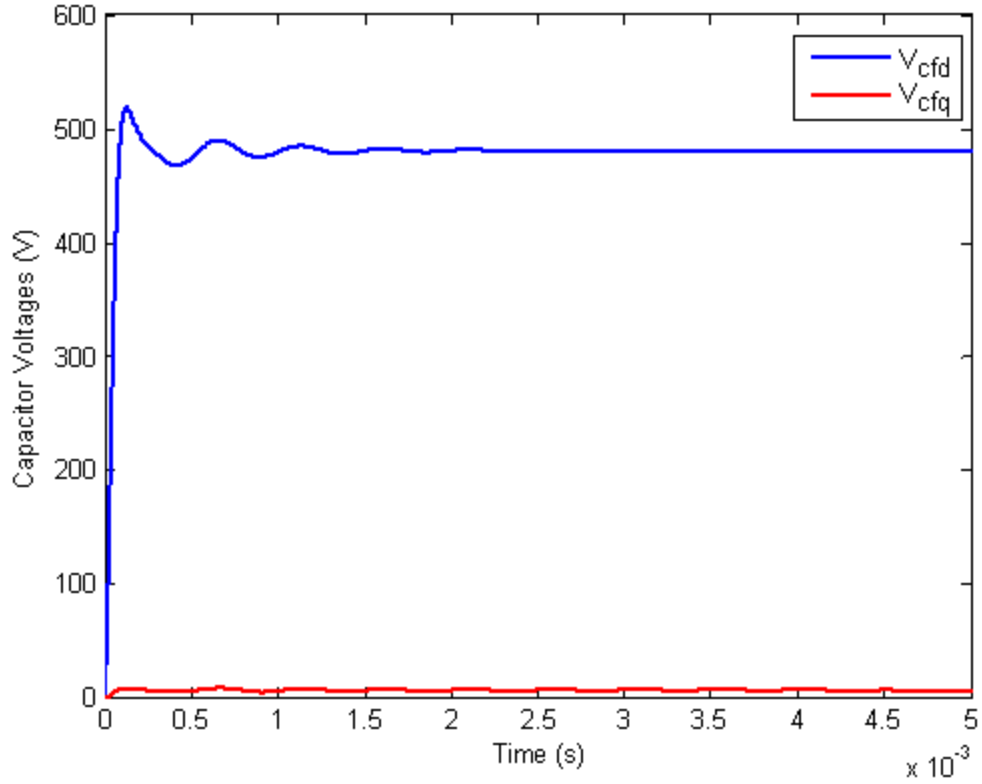
19

Figure 10.   LQG control with coherent noise.

The oscillations seen initially are due to differences between the estimated sinusoid and the actual disturbance. When the estimation converges, it completely cancels the disturbance sinusoid. The coherent noise disturbance given at the input of the plant is shown in Figure 11.

The speed of convergence can be controlled by the two noise covariances, as mentioned in the previous section. Eventually, it is a compromise between noise sensitivity and steady-state error, due to measurement noise and parameter variations. The noise covariances will need to be selected based on system performance during implementation.
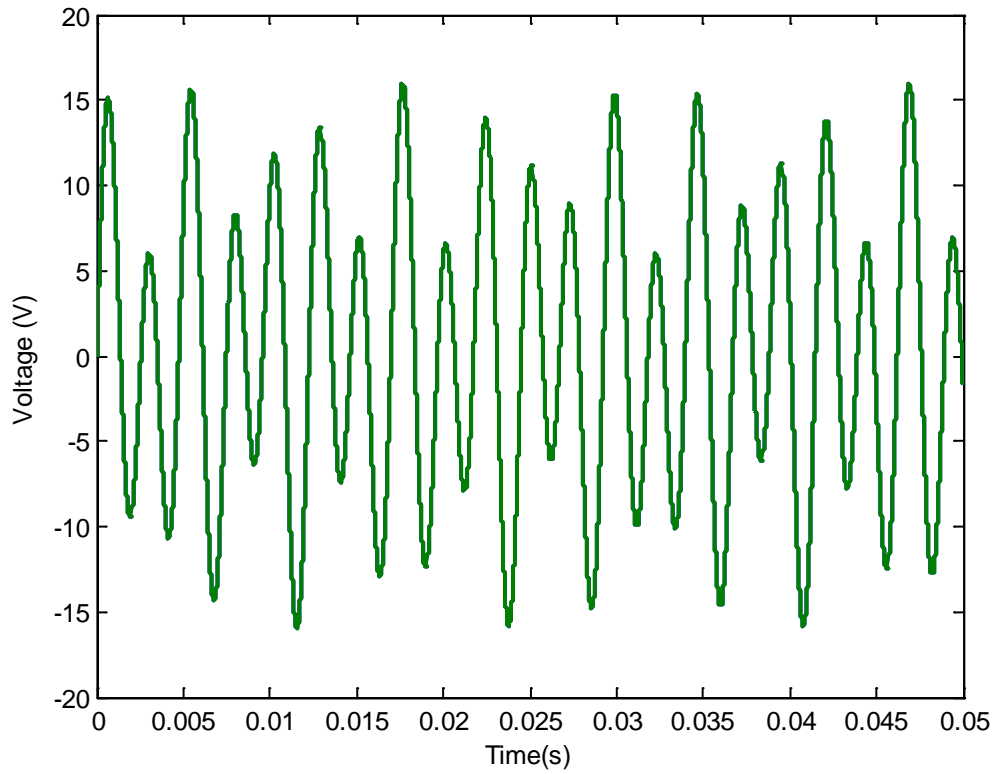
20

Figure 11.   Disturbance input to plant.

D.   LQG CONTROL WITH COHERENT NOISE AND WHITE NOISE

When white noise is added to both the sinusoidal disturbance and the measurement input to the Kalman filter, the system performance degrades. However, the noise is additive white Gaussian noise and not of the coherent nature that is the subject of this thesis.
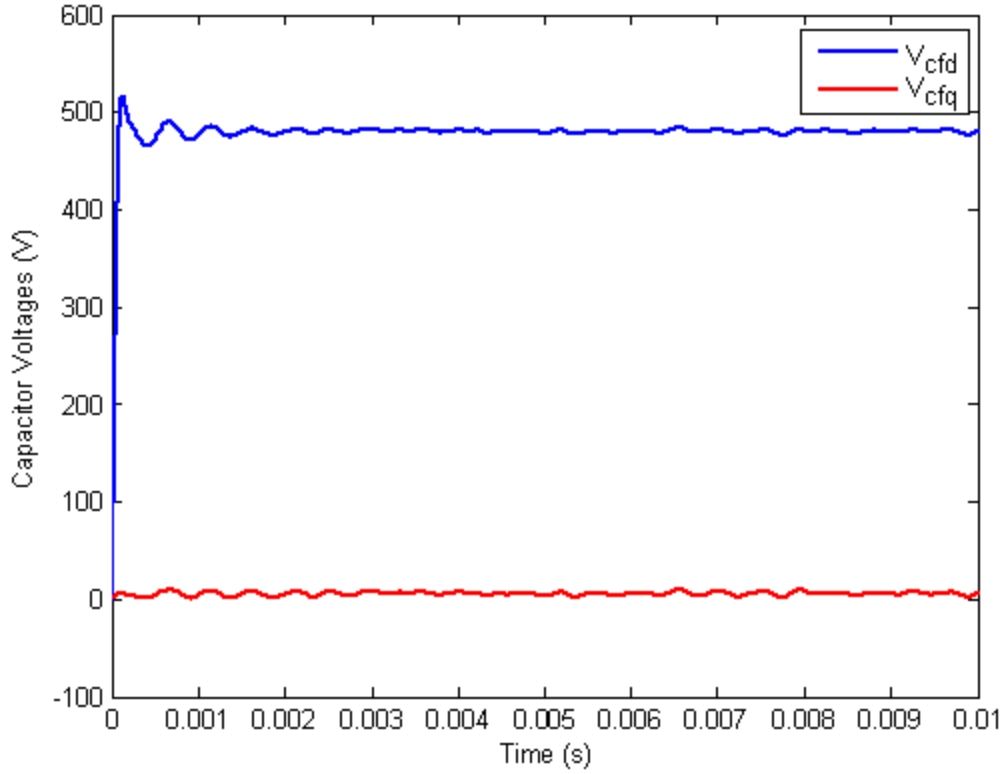
21

Figure 12.   LQG control with white noise.

The system operating under a high level of measurement noise and disturbance noise is shown in Figure 12. Noticeable ripples in the steady-state value can be seen. The measured value given to the observer for V_{cfq}, which has voltage variations as large as 30 V on the sensor, is shown in Figure 13. This is much larger than the noise specifications given in the datasheet for the sensor used, which is 1 percent, or 4.8V in this case. The datasheet for the voltage sensor used is provided in Appendix C.
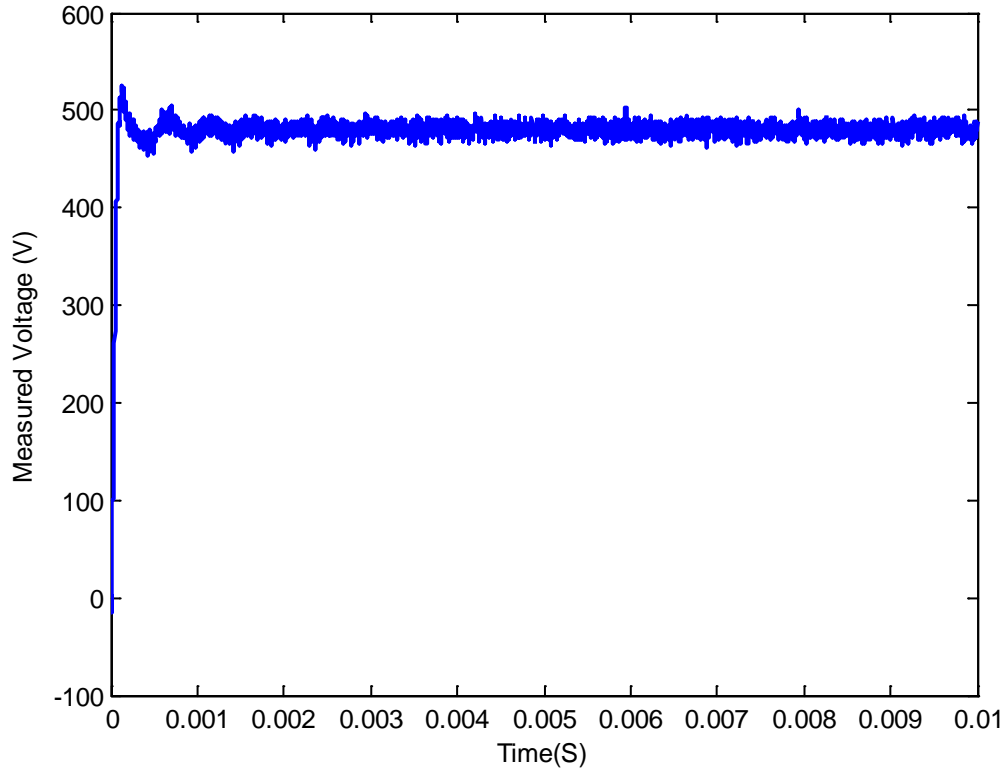
Figure 13.   Measured capacitor voltage with a high level of noise.

It is interesting to see how the parameters of the controller and the Kalman Filter affect the frequency response of the overall system. In particular, we are interested in the behavior of the system from the entry point of the disturbances to the output voltages of the system.

The frequency response can be obtained by a simple manipulation of the state space equations. In particular, combining the states of the systems and the observer, we obtain the state space model given by

$$
\begin{bmatrix} \dot{x} \\ \dot{\hat{x}} \end{bmatrix} = \begin{bmatrix} A_{Plant} & B_{plant}(-K-P) \\ GC_{plant} & A_{observer} - B_{observer}(K+P) - GC_{observer} \end{bmatrix} \begin{bmatrix} x \\ \hat{x} \end{bmatrix} + \begin{bmatrix} B \\ 0 \end{bmatrix} S
$$

$$
y = [C_{Plant} \quad 0] \begin{bmatrix} x \\ \hat{x} \end{bmatrix}
$$

(29)

.

23

The frequency responses for the two outputs are shown in Figure 14. The two plots refer to different parameter values of the system noise in the Kalman Filter. The system noise covariance is the only parameter changed. It is easy to see that, in all cases, as expected, the frequency response is zero at the two frequencies corresponding to the two harmonics. Furthermore, the effect of changing the value of the parameter can be seen on the width of the frequency null.

Since, in the actual system, there is a correlation between the harmonics, most likely the frequencies will not be exact and will be changing within a small range. In Equation (29), P represents a matrix that sums the estimated sinusoids in $\hat{x}$. This can then be used in the `bodemag()` command in MATLAB to generate a frequency response. The two lines shown represent two different variations of the system, one with a large weight of 200 on system noise and one with a small weight of 20.
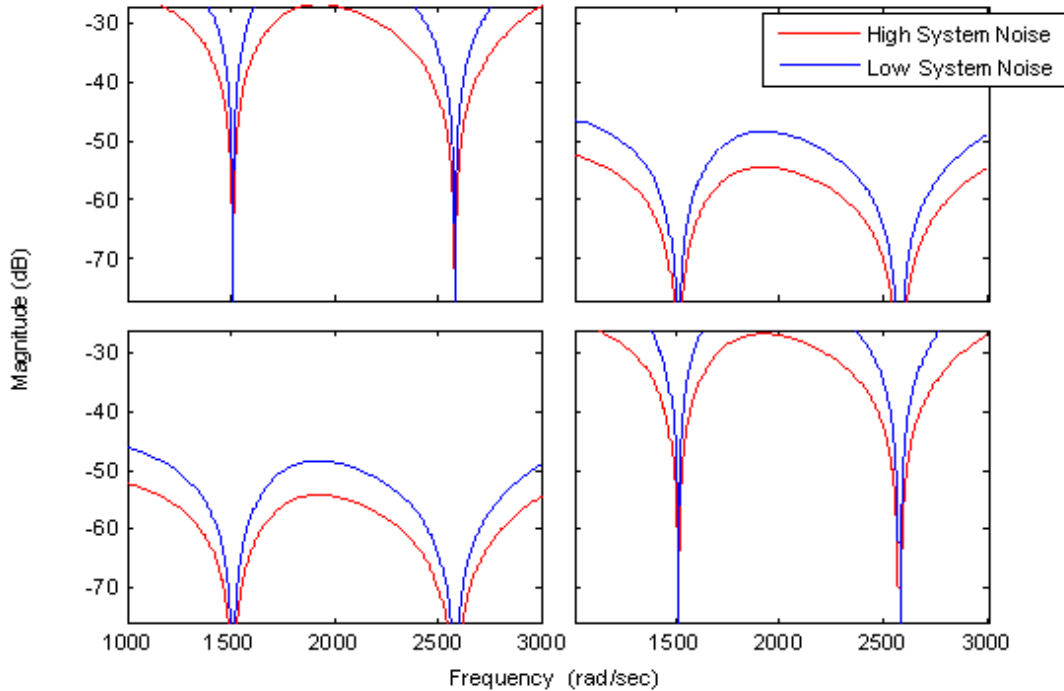

Figure 14.   Frequency response of closed loop system.

E.   LQG CONTROL WITH NOISE AND TIME DELAY

The addition of the time delay compensation, as discussed in Section II.C, has little effect on the system. However, it does introduce more instability because the controller is effectively using old measurements to calculate the desired system input. This most noticeably affects the transient response of the system. Since the nature of a power inverter is to be energized and to remain at steady-state for extended periods of time, the transient response is not something of critical interest.

The system response with a 100 microsecond time delay built into the system and the controller, as well as with white and coherent noise, is shown in Figure 15.
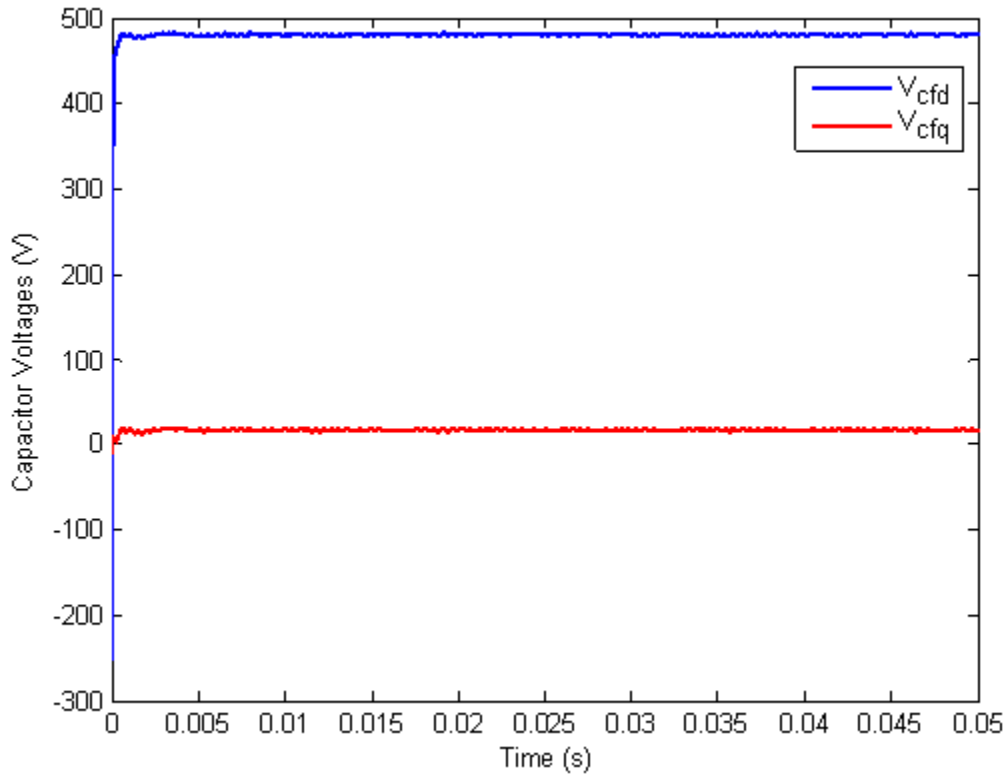

Figure 15.   System response with time delay.

This final simulation represents a fully functioning realistic controller, which can be implemented with a digital processor on a three-phase power inverter to effectively reject system coherent noise.

V. CONCLUSIONS AND FURTHER RESEARCH

A. CONCLUSIONS

By applying modern control theory to use an LQG controller as an active feedback filter in a power inverter, we can reject coherent noise at specific frequencies very effectively. This could be cost saving, removing the need for large, expensive, passive filters and allowing for smaller converters. This concept also leaves room for improvement, which can be done easily with a software update instead of having to retrofit hardware components. One controller can be applied to any number of systems and tuned for each specific system in software instead of requiring different hardware for each power converter.

B. FURTHER WORK

1. Implementation

This system has been proven to work in simulation; however, it still needs to be implemented in hardware. Using a digital processor, such as an FPGA, we can apply this controller to a standard power inverter and compare the results to the simulation results.
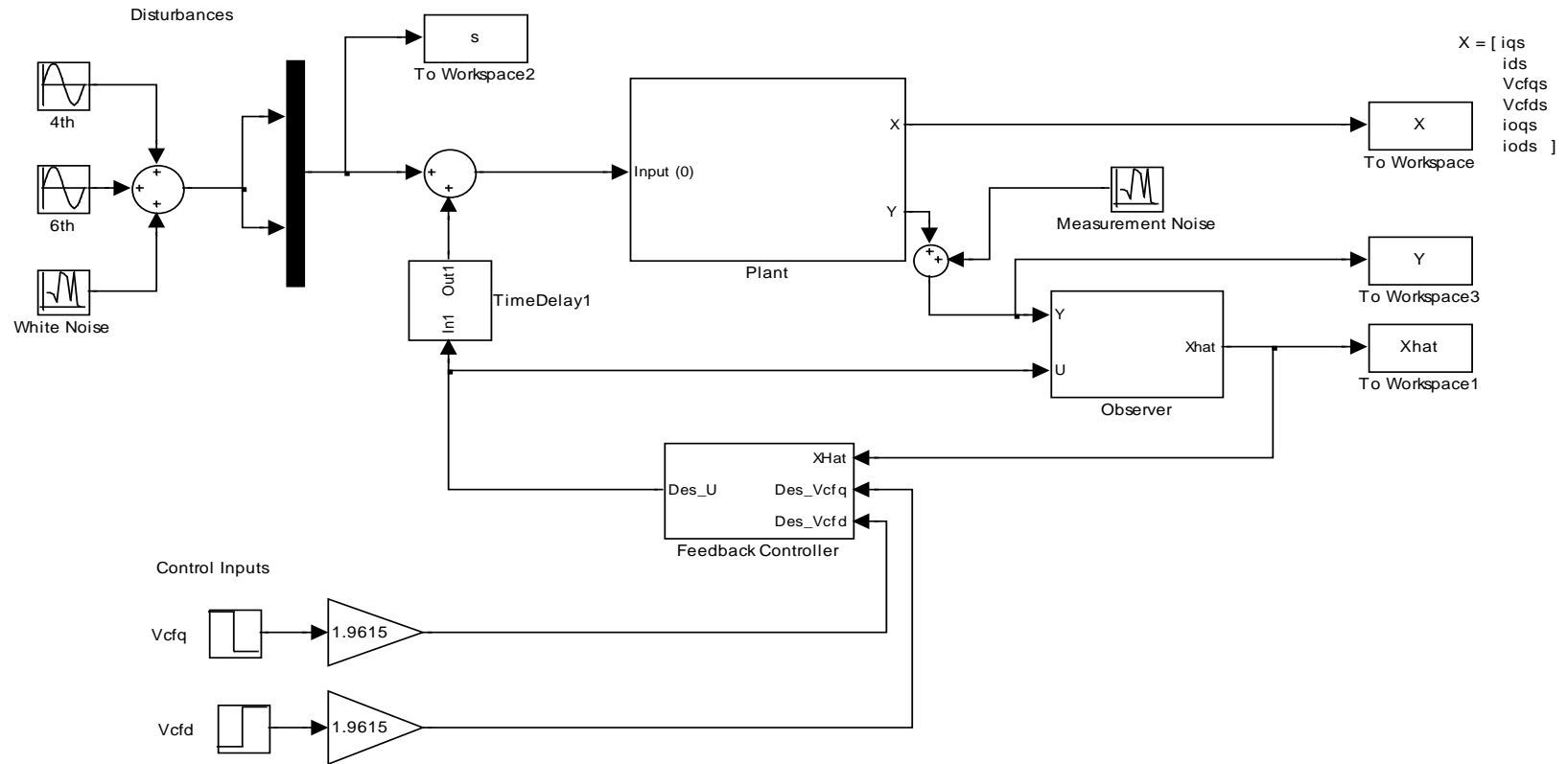
2. Optimization

The four weights in the LQR and Kalman filters were chosen based on the general performance of the system. The system performance could be enhanced with more careful selection of weights on the system states, control effort, plant noise, and measurement noise in the controller.

The algorithm presented can be improved in a number of ways. In particular, it can be made adaptive to be more effective in situations where the frequency changes with operating conditions. In particular, an adaptive filter could provide disturbance rejection by feedforward compensation, while the LQG controller, without the sinusoidal states, would provide the necessary stabilization.

27

THIS PAGE INTENTIONALLY LEFT BLANK

APPENDIX A. SIMULINK SCHEMATIC

Disturbances

4th

6th

White Noise

To Workspace2

s

Plant

Input (0)

X

Y

Measurement Noise

$X = [\ iqs$
ids
$Vcfqs$
$Vcfds$
$ioqs$
$iods\ ]$

X

To Workspace

Y

To Workspace3

Xhat

To Workspace1

TimeDelay1

Out1

In1

Observer

Y

U

Xhat

Feedback Controller

XHat

Des_U

Des_Vcfq

Des_Vcfd

Control Inputs

Vcfq

1.9615

Vcfd

1.9615

THIS PAGE INTENTIONALLY LEFT BLANK

APPENDIX B. SIMULINK INITIALIZATION CODE

```matlab
%SS Plant IC's
clear

T = 100e-6; %100microsecond delay in computation
Lf = 400e-6;
Cf = (6.6+8.8)*1e-6;
Lo = 30e-6;
Ro = 40;
w = 2*pi*60;


M = [0      w*Lf    1      0      0      0
    -w*Lf    0      0      1      0      0
    -1       0      0     w*Cf    1      0
     0      -1    -w*Cf    0      0      1
     0       0     -1      0      Ro    w*Lo
     0       0      0     -1    -w*Lo   Ro ];

N = [Lf     0      0      0      0      0
     0      Lf     0      0      0      0
     0      0      Cf     0      0      0
     0      0      0      Cf     0      0
     0      0      0      0      Lo     0
     0      0      0      0      0     Lo];

 P = [1      0
      0      1
      0      0
      0      0
      0      0
      0      0];



A = -N^-1 * M;
B = -N^-1 * P;
C = [eye(4), zeros(4,2)];

Q = eye(8);    % Q is weight on states
Q(3,3) = 5000;
Q(4,4) = 5000;
R = eye(2);    % R is weight on control effort

At = [A B
      zeros(1,6) -2/T 0
      zeros(1,7) -2/T];

Bt = [-B
```

```
      4/T 0
      0 4/T];


K = lqr(At,Bt,Q,R);


Bp = [zeros(8,2);Bt];




W = 20*eye(16);  %W is weight on plant  noise
V = eye(4);      %V is weight on sensor noise



C2 = [zeros(4,8), C,zeros(4,2)];
%ADD FUNDAMENTAL NOISE
%states increase

w1 = 2*pi*240;  %(60*5)-60  5th harmonic
w2 = (2*pi*(60*7)-60);   %  7th harmonic


W1 = [0 1; -w1^2 0];
W2 = [0 1; -w2^2 0];



Cr = [0 1];
cbar = [Cr zeros(1,2) Cr zeros(1,2); zeros(1,2) Cr zeros(1,2) Cr];
Bbar=Bt*cbar;

Ao = [W1 zeros(2,14)
       zeros(2,2) W1 zeros(2,12)
       zeros(2,4) W2 zeros(2,10)
       zeros(2,6) W2 zeros(2,8)
       Bbar At];




G=lqe(Ao,eye(16),C2,W,V);
```

APPENDIX C. DATASHEET FOR VOLTAGE SENSOR

Burr-Brown Products from Texas Instruments

ISO124

Precision Lowest-Cost ISOLATION AMPLIFIER

FEATURES

- 100% TESTED FOR HIGH-VOLTAGE BREAKDOWN
- RATED 1500Vrms
- HIGH IMR: 140dB at 60Hz
- 0.010% max NONLINEARITY
- BIPOLAR OPERATION: $V_O = \pm 10V$
- DIP-16 AND SO-28
- EASE OF USE: Fixed Unity Gain Configuration
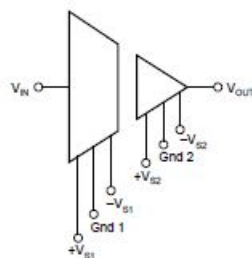- $\pm 4.5V$ to $\pm 18V$ SUPPLY RANGE

APPLICATIONS

- INDUSTRIAL PROCESS CONTROL: Transducer Isolator, Isolator for Thermocouples, RTDs, Pressure Bridges, and Flow Meters, 4-20mA Loop Isolation
- GROUND LOOP ELIMINATION
- MOTOR AND SCR CONTROL
- POWER MONITORING
- PC-BASED DATA ACQUISITION
- TEST EQUIPMENT

DESCRIPTION

The ISO124 is a precision isolation amplifier incorporating a novel duty cycle modulation-demodulation technique. The signal is transmitted digitally across a 2pF differential capacitive barrier. With digital modulation, the barrier characteristics do not affect signal integrity, resulting in excellent reliability and good high-frequency transient immunity across the barrier. Both barrier capacitors are imbedded in the plastic body of the package.

The ISO124 is easy to use. No external components are required for operation. The key specifications are 0.010% max nonlinearity, 50kHz signal bandwidth, and 200μV/°C V_{OS} drift. A power supply range of $\pm 4.5V$ to $\pm 18V$ and quiescent currents of $\pm 5.0mA$ on V_{S1} and $\pm 5.5mA$ on V_{S2} make these amplifiers ideal for a wide range of applications.

The ISO124 is available in DIP-16 and SO-28 plastic surface mount packages.

TEXAS INSTRUMENTS
www.ti.com

THIS PAGE INTENTIONALLY LEFT BLANK

LIST OF REFERENCES

[1]   H. W.Van Der Broeck, H.-C. Skudelny, G. V.Stanke, "Analysis and Realization of a Pulsewidth Modulator Based on Voltage Space Vectors," *IEEE Transactions on Industry Applications*, vol. 24, no. 1. Jan 1988.

[2]   Military Standard, "Interface Standard for Shipboard Systems Section 300A" *MIL-STD-1399 (Navy)*, 13 October 1987.

[3]   P. C. Krause, O. Wasynczuk, and S. D. Sudhoff, "Analysis of Electric Machinery and Drive Systems," *Second Edition IEEE Press,* pp. 109–133, 2002.

[4]   A. L. Julian, "EC4150 Derivation of State Space Model," Class notes for Power Electronics, Naval Postgraduate School, Monterey, CA, Winter 2011 (unpublished).

[5]   J. B. Burl, *Linear Optimal Control*. Boston: Addison Wesley Longman, Inc., pp.179–326, 1999.

[6]   N. S. Nise, *Control Systems Engineering*. Boston: Hoboken John Wiley & Sons, Inc., 2008.

[7]   N. Mohan, T. M. Undeland, and W. P. Robbins. *Power Electronics: Converters, Applications and Design*. Hoboken: John Wiley & Sons, Inc., 2003.

[8]   D. G. Holmes, "The Significances of Zero Space Vector Placement for Carrier-Based PWM Schemes," *IEEE Transactions on Industry Applications* vol. 32, no. 5. September/October 1996.

THIS PAGE INTENTIONALLY LEFT BLANK

INITIAL DISTRIBUTION LIST

1. Defense Technical Information Center
   Ft. Belvoir, Virginia

2. Dudley Knox Library
   Naval Postgraduate School
   Monterey, California

3. Dr. Clark Robertson
   Naval Postgraduate School
   Monterey, California

4. Dr. Roberto Cristi
   Naval Postgraduate School
   Monterey, California

5. Dr. Alexander Julian
   Naval Postgraduate School
   Monterey, California

6. ENS Daniel G. Wheaton
   U.S. Navy
   Old Town, Maine